Available online at www.sciencedirect.com

ScienceDirect

Nuclear Physics A 967 (2017) 27–34

NUCLEAR PHYSICS A

www.elsevier.com/locate/nuclphysa

Overview of recent results from HADES

Manuel Lorenz for the HADES collaboration

Institut für Kernphysik, Goethe-Universität, 60438 Frankfurt, Germany
m.lorenz@gsi.de

Abstract

HADES is a multi-purpose charged-particle detector operated at the SIS18 synchrotron located at the GSI Helmholtz Center for Heavy Ion Research in Darmstadt, Germany. The provided ion beam energies of 1-2 A GeV are the lowest of all currently running heavy-ion experiments and result in the highest baryo-chemical potentials at freeze-out in case of Au+Au collisions. At this Quark Matter conference we presented results from Au+Au collisions at $\sqrt{s_{NN}}$ = 2.4 GeV. The created system exhibits a very clear hierarchy in hadron yields, with about 100 protons, 10 pions, 10^{-2} kaons and 10^{-4} antikaons per event. The HADES program focuses on four main observables: (subthreshold) strangeness production, particle flow and its anisotropies, virtual photon emission and net-proton number fluctuations.

Keywords: HADES, QCD-phase diagram, high μ_B, GSI, SIS18, subthreshold, strangeness, charged kaon freeze-out, flow anisotropies, virtual photon emission, net-proton fluctuations

1. HADES and the Baryon-Rich Side of the QCD Phase Diagram

The characterizations of physical properties of strongly interacting matter in its different phases is one of the challenges of modern physics. Especially, at high net-baryon densities properties of QCD matter are not well established. Due to the fermion determinant sign problem [1], ab-initio calculations can not be preformed in this regime. Thus, one has to rely on extrapolations or models based on effective Lagrangians, which need to be confronted with experimental data.

Heavy-ion collisions (HIC) provide a unique tool for this enterprise. As both, the inter-penetration time of the colliding nuclei decrease with increasing collision energy, and the amount of stopped nucleons in the collision zone decreases, resulting in a systematic increase of net-baryon density in the collision zone with decreasing energy. On a more quantitative level the extracted freeze-out parameters from statistical hadronization model (SHM) fits [2, 3, 4] to particle yields obtained at various energies show a striking regularity, lining up on a curve in the temperature - baryo-chemical potential plane, connecting smoothly data from the lowest energies at SIS18 up to the highest available energy at LHC [5, 6]. This offers a unique possibility of a systematic scan of the different phases of strongly interacting matter in the laboratory.

HADES is a multi-purpose charged-particle detector operated at the SIS18 synchrotron located at the GSI Helmholtz Center for Heavy Ion Research in Darmstadt, Germany. The provided ion-beam energies of 1-2 A GeV translate to the highest baryo-chemical potentials at freeze-out [5] of all currently running heavy-ion experiments.

http://dx.doi.org/10.1016/j.nuclphysa.2017.06.010
0375-9474/© 2017 The Author(s). Published by Elsevier B.V.
This is an open access article under the CC BY license (http://creativecommons.org/licenses/by/4.0/).

HADES comprises a 6-coil toroidal magnet centered around the beam axis and six identical detection sections located between the coils, covering almost the full azimuthal angle. Each sector is equipped with a Ring-Imaging Cherenkov (RICH) detector followed by low-mass Mini-Drift Chambers (MDCs), two in front of and two behind the magnetic field, as well as a scintillator hodoscope (TOF) and a resistive plate chamber (RPC) at the end of the system. The RICH detector is used mainly for electron/positron identification, the MDCs are the main tracking detectors, while the TOF and RPC are used for time-of-flight measurements in combination with a diamond start detector located in front of a 15-folded segmented target. The setup is completed by a forward hodoscope used for event plane determination. A detailed description of the HADES detector is given in [7].
At this Quark Matter conference we presented results from Au+Au collisions at $\sqrt{s_{NN}} = 2.4$ GeV. The created system exhibits a very clear hierarchy in hadron yields, with about 100 protons, 10 pions, 10^{-2} kaons and 10^{-4} antikaons per event. In order to accumulate sufficient statistics for a multi-differential analysis, even of the most rarely produced hadrons like antikaons, a fast data acquisition is mandatory. In total about 4×10^9 Au+Au events corresponding to the 40% most central events [8], have been collected in a four week measuring campaign with average trigger rates of 8 kHz and a 50% duty cycle. Particles are identified based on the correlation between the time-of-flight and the momentum measurement. Additional separation power is gained by the energy-loss information from the MDCs and the TOF detector and in case of electron/positron identification based on the information of the dedicated RICH and Pre-shower detectors.
The HADES program focuses on four main observables: (subthreshold) strangeness production, particle flow and its anisotropies, virtual photon emission and net-proton number fluctuations; they are discussed successively below.

2. (Subthreshold) Strangeness Production

Hadrons carrying strangeness are promising probes of the system created in HIC and have relevance for various astrophysical processes. As kaons contain an anti-strange quark, their coupling to baryons via formation of resonances is suppressed and they propagate in nuclear matter at ground state densities relatively free. One can estimate their mean free path in nuclear matter to $\lambda \approx 5$ fm by applying the low density approximation to the measured K^+-N cross-section, as implemented in microscopic transport models [9].
On the other hand, the spectral function of antikaons is complicated due to their coupling to baryon-resonances and have attracted much attention since the possibility of a $\overline{K}$ condensate in dense nuclear matter was first discussed in the eighties of last century by Kaplan and Nelson [10]. Various approaches based on chiral Lagrangians [11], one-boson-exchange models [12], the Nambu-Jona-Lasino model [13] or coupled-channel calculations [14, 15, 16] predict an overall attractive $\overline{K}$-nucleon potential.
Hyperons, in addition, are of particular interest as their behavior influences the properties of the surrounding matter, as well. It has long been realized that inside neutron stars the appearance of hyperons is possible via the weak interaction and it substantially softens the equation of state (EOS) [17, 18, 19, 20]. This leads to an upper limit for the maximum neutron star mass, what creates tension [21, 22] with the recent observations of two solar mass neutron stars [23, 24]. Whether the appearance of hyperons inside a neutron star is energetically favorable depends on the strength of the Λ-nucleon potential, which is known to be attractive at ground state densities from hypernuclei formation [25]. However, the density dependence of the potential is vague [26]. Calculations based on the quark model in combination with a non-linear $\omega - \sigma$ model predict an attractive potential for densities below three times nuclear ground density but a repulsive potential for higher densities [27]. HIC are the unique tool to study the potentials between nucleons and hadrons carrying strangeness at high densities. Hence, numerous works focused on kaons in this energy regime in the past.
One of the most notable is the attempt to extract the equation of state (EOS) at densities exceeding nuclear ground state, based on the comparison of K^+ multiplicity ratios from heavy (Au+Au) to light (C+C) collision systems to the same quantity obtained from microscopic transport models [28, 29, 30].
In addition, the K-N potential has been frequently in the focus of investigations. Most of the comparisons of experimental data to microscopic models are also in favor of a repulsive K-N potential [31, 32, 33, 34, 9, 35, 36]. However, no complete picture of one model being able to describe all kaon observables consistently emerged yet [37, 38]. Note, that in a recent work by the UrQMD group, the uncertainty of the kaon spectra

shape was found to be large due to not well constrained resonance decays hampering any conclusions about the K-N potential [39].

The first high-quality data on subthreshold K^- production in relativistic heavy-ion collisions (HIC) have become available in the late 1990s [34, 40, 41]. The experimental data revealed a similar rise of K^+ and K^- yields with increasing centrality of the collision, and systematically softer K^- spectra compared to the ones of the K^+. The already in the early eighties by Ko [42] predicted strangeness exchange reaction, e.g. $\pi Y \rightarrow N\overline{K}$, was identified as the dominant source for subthreshold K^- production through detailed comparisons between the obtained data and transport models. As a consequence the K^- freezes out at later times compared to the K^+ within the models and hence also the softer spectra could be explained [43]. Attempting to extract the $\overline{K}$-N potential, most comparison between K^- heavy-ion data and transport models seem to favor a somewhat attractive $\overline{K}$-N potential. Quantitative conclusions remain however vague and under discussion [9, 38, 44].

In addition, newer data from the FOPI and HADES collaborations reveal that a sizable ($\approx$ 20%) fraction of the observed K^- yield results from ϕ decays [45, 46, 47, 48, 49]. Based on our data from [46] we were able to show that the observed difference in the slope of the K^+ and K^- spectra can be explained simply by taking the K^- contribution from ϕ decays into account, as those K^- have substantially softer spectra [50]. This trend was later confirmed by the FOPI collaboration [47, 48, 49].

Recently, feed-down from higherlying baryonic resonances have been included in UrQMD in order to be able to describe the energy dependence of the ϕ/K^- ratio also in a transport code [51]. The authors tuned the mass depended branching ratios of higher lying baryonic resonances, namely the $N^*(1990)$, $N^*(2080)$, $N^*(2190)$, $N^*(2220)$ and $N^*(2250)$, to match elementary data on ϕ meson production [52]. As a result, the ϕ/K^- in Ar+KCl is successfully reproduced, as well as the trend of the excitation function at low energies.

Data on hyperon production from HIC at low energies are scarce. While at SIS18 energies only data from medium-sized collision systems are available [53, 54], at AGS energies Λ production has been investigated in greater detail [55, 56, 57].

In addition, the yield of the deep-subthreshold production of the Ξ^- measured by HADES in Ar+KCl collisions at a kinetic beam energy of 1.76 A GeV, exceeds thermal model predictions by an order of magnitude [58, 59], can up to now, only be reproduced by one model [60] and is referred to as the Ξ^- puzzle.

In the presented collision system of Au+Au at $\sqrt{s_{NN}}$ = 2.4 GeV all hadrons carrying strangeness are produced below their free NN-threshold $\sqrt{s_{th}}$: -150 MeV for K^+, K^0, Λ and -450 MeV, -490 MeV for the K^- and the ϕ meson and can therefore not be formed directly in binary collisions. Hence, they are considered to be suitable messengers of the high-density phase of such collisions. Furthermore, it is the first measurement of all these hadrons so far below threshold, except for the K^+. While the experimental coverage in transverse momentum extends down to almost zero, K^0, Λ are ideal for testing the effect of the potential. This will be one of the focuses of a future publication. In this contribution, we focus on the results and effects discussed in [61], where the ϕ/K^- ratio is found to be 0.52 ± 0.16 and hence resonant K^- production via ϕ mesons turns out to be a sizable source of antikaon production at subthreshold energies.

2.1. Implications for the sequential freeze-out of charged kaons

In order to investigate the effect of the ϕ feed-down on the observed slope of the K^- spectra as discussed in [61], which in the past has been interpreted as experimental evidence for a sequential freeze-out of kaons and antikaons, we build a two-component model using the event generator Pluto [62], starting from the simplest assumption that both kaon species are emitted with the same thermal source (resulting in similar momentum distributions). For this, we use a static thermal source with a temperature of T=104 MeV according to the measured inverse slope of the K^+. In addition we generate ϕ mesons as a second thermal source characterized by the measured inverse slope of the ϕ mesons of T=108 MeV. Note, that due to the hierarchy in production yields the effect on the K^+ spectra is negligible. In case of the K^- however, we scale the two contributions of direct and resonantly produced K^- according to the measured ϕ/K^- ratio of 0.52 ± 0.16. The resulting sum of both contributions is then fitted using the following equation:

$$\frac{1}{m_t^2}\frac{d^2M}{dm_t dy_{cm}} = C(y_{cm})\,\exp\left(-\frac{(m_t - m_0)}{T_B(y_{cm})}\right). \tag{1}$$

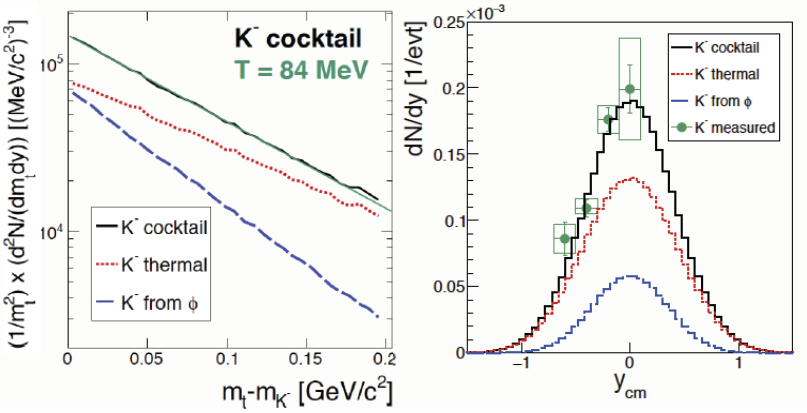

Fig. 1. Left: Simulated transverse mass spectra of K^-: Direct thermal (red), resulting from ϕ decays (blue), sum of both (black). In addition a fit using Eq. 1 in a similar $m_t - m_0$ range between 0 and 200 MeV/c^2 as used for the real data is displayed in (green). The extracted slope of (84 ± 5) agrees perfectly with the measured slope of K^- of (84 ± 6) MeV, see text for details. Right: Comparison of the experimental dN/dy spectrum to the two-component model (black).

in a similar $m_t - m_0$ range between 0 and 200 MeV/c^2 as applied for real data. In this contribution we visualize the effect on the spectra in addition to the information already given in reference [61], further additional information on the centrality dependence of the discussed contribution are given in [63] within these proceedings. The different contributions and the corresponding Boltzmann fit are displayed on the left panel in Fig. 1. The extracted slope of (84 ± 5) MeV agrees with the measured slope of K^- of (84 ± 6) MeV. The error is obtained by variation of the ϕ/K^- ratio within the given errors. Note that the error on the inverse slope parameter of the experimental spectra is propagated by making use of the covariance matrix already when determining the total production and hence is not varied explicitly again. Not only the slope of the spectra is described by the two-component model, also the shape of the rapidity distribution is reproduced, displayed together with the K^- data on the right panel of Fig. 1. While the lowering of the slope was already indicated from similar investigations in smaller systems at higher energies [50, 47, 48, 49] one expects that K^- production far below the free NN threshold and in a large collision system the relative strength of resonant K^- production compared to strangeness exchange reactions to diminish and hence the simple two-component model to fail describing the experimental observations. However, we observe quite the opposite behavior, we do find not only good agreement between the measured and simulated slope, we also find agreement for the shape of the rapidity distributions. Hence, we conclude that, although there is still room for strangeness exchange reactions to occur within experimental errors, according to Occam's razor, the simplest assumption of the direct and resonant K^- production is the presumable picture to explain the different slopes of charged kaons at SIS energies. This implies, that the most prominent experimental signature for sequential freeze-out of kaons and antikaons is obsolete.
The different slopes of the K^+ and K^- spectra can be fully explained by feed-down of ϕ mesons. As a direct consequence, attempts to extract the K^--N potential and all further conclusions based on it e.g. for astrophysical objects or general properties of QCD matter need to be revisited.

3. Particle flow and its Anisotropies

Using particle flow patterns one can constrain the equation of state [64], extract transport properties or estimate initial state fluctuations in the investigated system. The azimuthal angular anisotropy in particle production can be characterized by the Lorentz invariant Fourier decomposition:

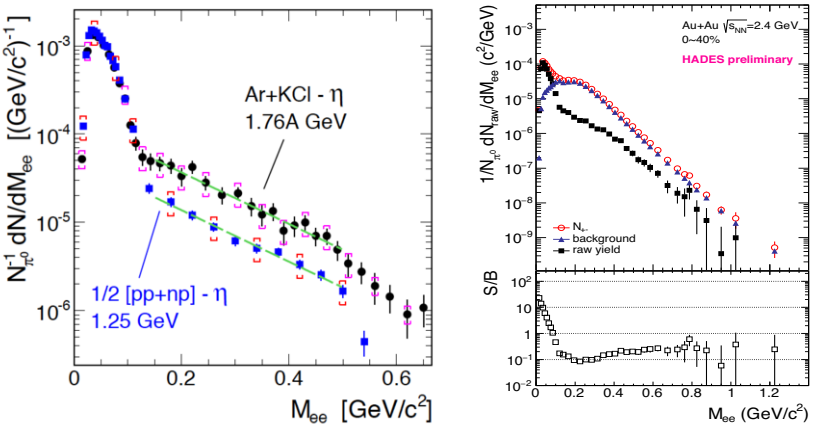

Fig. 2. Left: Comparison of the Ar+KCl invariant-mass distribution with an isospin-averaged reference from p+p and n+p data [72, 73]. For clarity systematic error bars are shown only on every second data point (vertical bars are statistical, cups are systematic). Both data sets are normalized to their respective pion multiplicity and have their respective η Dalitz yield subtracted. The dashed lines are meant to guide the eye. Right: The new invariant mass distribution reconstructed from Au+Au collisions at 1.23 A GeV. The corresponding signal to background ratio is displayed in the lower part of the figure.

$$E\frac{d^3N}{d^3\mathbf{p}} = \frac{1}{2\pi}\frac{d^2N}{p_t dp_t dy}\{1 + \sum_n 2v_n cos\left[n(\phi - \Psi_{RP})\right]\} \tag{2}$$

where E is the particle energy, p_t the transverse momentum, y the rapidity, and Ψ_{RP} the reaction plane angle (spanned by the impact parameter and the beam axis). The reaction plane must be reconstructed from particle emission and is called event plane in the traditional method.

At RHIC and LHC energies various analysis focus on the higher flow harmonics [65, 66], which have been shown to be sensitive to the initial state fluctuations as well as to transport coefficients of the created medium.

Published flow pattern of particles at SIS energies are restricted to the first and second moment v_1 and v_2, however with the high statistics of collected Au+Au collisions the investigation of higher order flow harmonics becomes possible.

In this conference we presented results of proton v_1 and v_2 [67], which can be used as standard candles to validate the reconstruction before extending the investigations to higher moments. In addition also newer techniques, like the cumulants method, which are a measure of multi-particle correlations, will be exploited. The method allows to estimate flow effects without the knowledge of the angle Ψ_{RP} and having additionally the feature of a suppression of non-flow contributions, like resonance decays, for higher moments [68]. Similar as for the higher harmonics, no flow pattern based on this method are published for SIS energies, with one exception [69].

4. Virtual Photon Emission

Virtual photon emission transports direct information from the fireball created in heavy-ion collisions and can be reconstructed using lepton pairs. The shape of the invariant mass spectrum reveals directly hadron properties like position medium widths and pole position of vector mesons, as the signal is not distorted by strong final state interactions. The shape can be also used as a thermometer and the strength of the radiation reveals information about the lifetime of the created system [70, 71].

Experimentally however, dilepton measurements are extremely challenging as apart from the small branching ratio of the electromagnetic decay of order 10^{-4} and large combinatorial background, one has to disen-

tangle several broad and overlapping contributions in the reconstructed spectrum.
Comparisons of the strength of dielectron radiation from p+p and n+p reactions at a kinetic beam energy of 1.25 GeV measured with HADES, revealed a strong isospin effect [72]. Hence, one has to compare the dielectron yield from heavy-ion data to an elementary reference consisting of radiation from both p+p and n+p collisions.
Comparing the dielectron yield from Ar+KCl collisions at a kinetic beam energy of 1.76 A GeV, normalized to the neutral pion multiplicity, in the invariant mass region between 0.15 GeV/c^2 and 0.5 GeVc^2 to such an elementary reference a strong excess is observed, see left side of Fig. 2 (the energy dependence is taken out to some extent due to the normalization) [73]. The new invariant mass distribution reconstructed from Au+Au collisions at 1.23 A GeV is shown in Fig. 2 (right). The corresponding signal to background ratio is displayed in the lower part. The numbers of e^+e^- pairs in the mass range 0.15-0.55 GeVc^2 is about $\approx 1.4 \times 10^4$ and allows for multi-differential analysis.
A similar comparison for data from the first heavy collision system (Au+Au) in this energy regime was presented and will be discussed in a contemporary publication [74].

5. Net-proton fluctuations

Another very promising observable, in particular for mapping out the QCD phase diagram are higher moments of conserved quantities like the baryon number, as they could be connected to critical fluctuations expected near an end point in the phase diagram [75].
Due to the experimental challenges in reconstructing neutrons, one usually uses the protons as a proxy for the baryons. At low energies the situation is complicated further as a large fraction of protons is bound in light nuclei, which might have to be also reconstructed or corrected for. In addition, due to the absence of antiprotons no terms chancel, when it comes to volume fluctuations in the determination of the centrality classes [76].
Furthermore, as the proton multiplicity distributions have to be corrected for the detector response, these measurements are sensitive to all kind of detector effects. Thus, such measurements have to be handled with detailed systematic studies of those effects based on simulations, in order to achieve meaningful results. Some of the lessons learned during this endeavor are discussed in [77], the rest together, with results of Au+Au data are subject to another contemporary publication [78], including also a comparison to recently published data from the STAR collaboration [79]. For such a comparison it is important to consider the phase space window, in which the distributions are measured. In general, the window must not be too large as otherwise contributions from spectator matter enter and on the other hand not to small as otherwise the Poisson limit is approached [80, 81]. As HADES is a fixed target experiment and in addition, the spectator matter is not as well separated in rapidity as at RHIC energies, the used rapidity window Δy is smaller than the one used in the STAR analysis.
We have presented the first results on net-proton fluctuations in this energy regime at the conference. The question how to best compare results from largely different beam energies is still actively discussed. Both will be subject to a contemporary publication.

References

[1] O. Philipsen, EPJ Web Conf. **137** 03016 (2017).
[2] P. Braun-Munzinger, K. Redlich and J. Stachel, arXiv:nucl-th/0304013 (2003).
[3] A. N. Tawfik, Int. J. Mod. Phys. A **29** 17, 1430021 (2014).
[4] M. Floris, Nucl. Phys. A **931** 103 (2014).
[5] J. Cleymans, H. Oeschler, K. Redlich and S. Wheaton, Phys. Rev. C **73**, 034905 (2006).
[6] J. Stachel, A. Andronic, P. Braun-Munzinger andK. Redlich, J. Phys. Conf. Ser. 509, 012019 (2014).
[7] G. Agakishiev *et al.* [HADES Collaboration], Eur. Phys. J. A **41**, (2009) 243.
[8] B. Kardan, Diploma Thesis, Goethe-University Frankfurt (2016).
[9] C. Hartnack, H. Oeschler, Y. Leifels, E. L. Bratkovskaya, J. Aichelin, Phys. Rept. **510** (2012) 119.
[10] D. B. Kaplan and A. E. Nelson, Phys. Lett. B **175** (1986) 57.
[11] C. H. Lee, G. E. Brown, D. P. Min and M. Rho, Nucl. Phys. A **585** (1995) 401.
[12] J. Schaffner-Bielich, J. Bondorf, A. Mishustin, Nucl. Phys. A **625**, (1997) 325.

[13] M. F. M. Lutz, A. Steiner and W. Weise, Nucl. Phys. A **574** (1994) 755.
[14] V. Koch, Phys. Lett. B **337** (1994) 7.
[15] W. Cassing, E. L. Bratkovskaya, U. Mosel, S. Teis, A. Sibirtsev, Nucl . Phys. A **614** (1997) 415.
[16] D. Cabrera, L. Tolos, J. Aichelin and E. Bratkovskaya, J. Phys. Conf. Ser. **668** (2016) no.1, 012048.
[17] V. R. Pandharipande, Nucl. Phys. A **178** (1971) 123.
[18] H. A. Bethe and M. B. Johnson, Nucl. Phys. A **230** (1974) 1.
[19] N. K. Glendenning and S. A. Moszkowski, Phys. Rev. Lett. **67** (1991) 2414.
[20] S. Balberg and A. Gal, Nucl. Phys. A **625** (1997) 435.
[21] A. W. Thomas *et al.*, EPJ Web of Conferences **63**, (2013) 03004.
[22] M. Buballa *et al.*, J. Phys. G **41** (2014) no.12, 123001
[23] P. Demorest *et al.*, Nature **476**, (2010) 1081.
[24] J. Antoniadis *et al.*, Science **340**, (2013) 6131.
[25] C. J. Batty, E. Friedman and A. Gal, Phys. Rept. **287** (1997) 385.
[26] S. Weissenborn, D. Chatterjee and J. Schaffner-Bielich, Nucl. Phys. A **881** (2012) 62.
[27] Z. S. Wang, A. Faessler, C. Fuchs and T. Waindzoch, Nucl. Phys. A **645** (1999) 177, Erratum: [Nucl. Phys. A **648** (1999) 281].
[28] C. T. Sturm *et al.* [KAOS Collaboration], Phys. Rev. Lett. **86** (2001) 39
[29] C. Fuchs, A. Faessler, E. Zabrodin and Y. M. Zheng, Phys. Rev. Lett. **86** (2001) 1974.
[30] C. Hartnack, H. Oeschler and J. Aichelin, Phys. Rev. Lett. **96** (2006) 012302
[31] M. L. Benabderrahmane *et al.* [FOPI Collaboration], Phys. Rev. Lett. **102** (2009) 182501.
[32] G. Agakishiev *et al.*, [HADES Collaboration], Phys. Rev. C **82** (2010) 044907.
[33] G. Agakishiev *et al.* [HADES Collaboration], Phys. Rev. C **90** (2014) 054906.
[34] A. Förster, F. Uhlig, I. Bottcher, D. Brill, M. Debowski *et al.*, Phys. Rev. C **75** (2007) 024906.
[35] A. Mishra, E. L. Bratkovskaya, J. Schaffner-Bielich, S. Schramm and H. Stoecker, Phys. Rev. C **70** (2004) 044904.
[36] S. Pal, C. M. Ko, Z. w. Lin and B. Zhang, Phys. Rev. C **62** (2000) 061903.
[37] V. Zinyuk *et al.* [FOPI Collaboration], Phys. Rev. C **90** (2014) no.2, 025210.
[38] C. Fuchs, Prog. Part. Nucl. Phys. **56** (2006) 1.
[39] J. Steinheimer and M. Bleicher, EPJ Web Conf. **97** (2015) 00026.
[40] F. Laue *et al.* [KaoS Collaboration],Phys. Rev. Lett. **82** (1999) 1640.
[41] M. Menzel *et al.* [KaoS Collaboration], Phys. Lett. B **495** (2000) 26.
[42] C. M. Ko, Phys. Lett. B **120** (1983) 294.
[43] C. Hartnack, H. Oeschler and J. Aichelin, Phys. Rev. Lett. **90** (2003) 102302.
[44] W. Cassing, L. Tolos, E. L. Bratkovskaya and A. Ramos, Nucl. Phys. A **727** (2003) 59.
[45] A. Mangiarotti *et al.* [FOPI Collaboration], Nucl. Phys. A **714** (2003) 89.
[46] G. Agakishiev *et al.* [HADES Collaboration], Phys. Rev. C **80** (2009) 025209.
[47] K. Piasecki *et al.* [FOPI Collaboration], Phys. Rev. C **91**, (2015) 054904.
[48] P. Gasik *et al.* [FOPI Collaboration], Eur. Phys. J. A **52** (2016) 177.
[49] K. Piasecki *et al.* [FOPI Collaboration], Phys. Rev. C **94** (2016) 014901.
[50] M. Lorenz *et al.* [HADES Collaboration], PoS (BORMIO2010) (2010) 038.
[51] J. Steinheimer and M. Bleicher, J. Phys. G **43** 1, (2016) 015104.
[52] Y. Maeda *et al.* [ANKE Collaboration], Phys. Rev. C **77** (2008) 015204.
[53] N. Bastid *et al.* [FOPI Collaboration], Phys. Rev. C **76** (2007) 024906.
[54] G. Agakishiev *et al.* [HADES Collaboration], Eur. Phys. J. A **47** (2011) 21.
[55] C. Pinkenburg *et al.* [E895 Collaboration], Nucl. Phys. A **698** (2002) 495.
[56] P. Chung *et al.*, Phys. Rev. Lett. **86** (2001) 2533.
[57] S. Albergo *et al.*, Phys. Rev. Lett. **88** (2002) 062301.
[58] G. Agakishiev *et al.* [HADES Collaboration], Phys. Rev. Lett. **103** 132301 (2009).
[59] J. Steinheimer, T. Lang, H. van Hees, A. S. Botvina et al., J. Phys. Conf. Ser. **509** 012002 (2014).
[60] F. Li, L. -W. Chen, C. M. Ko and S. H. Lee, Phys. Rev. C **85** 064902 (2012).
[61] J. Adamczewski-Musch *et al.* [HADES Collaboration], arXiv:1703.08418 [nucl-ex].
[62] I. Fröhlich *et al.*, J.Phys. Conf. Ser. 219 (2010) 032089.
[63] H. Schuldes *et al.* [HADES Collaboration], these proceedings.
[64] P. Danielewicz, R. Lacey and W. G. Lynch, Science **298** (2002) 1592.
[65] L. Adamczyk *et al.* [STAR Collaboration], arXiv:1701.06497 [nucl-ex].
[66] K. Aamodt *et al.* [ALICE Collaboration], Phys. Rev. Lett. **107** (2011) 032301.
[67] B. Kardan *et al.* [HADES Collaboration], these proceedings.
[68] S. A. Voloshin, A. M. Poskanzer and R. Snellings, in Landolt-Boernstein, Vol. **1/23**, p. 5-54 (Springer-Verlag, 2010).
[69] N. Bastid *et al.* [FOPI Collaboration], Phys. Rev. C **72** (2005) 011901.
[70] R. Rapp and H. van Hees, Phys. Lett. B **753** (2016) 586.
[71] T. Galatyuk, P. M. Hohler, R. Rapp, F. Seck and J. Stroth, Eur. Phys. J. A **52** (2016) no.5, 131.
[72] G. Agakishiev *et al.* [HADES Collaboration], Phys. Lett. B **690** (2010) 118.
[73] G. Agakishiev *et al.* [HADES Collaboration], Phys. Rev. C **84** (2011) 014902.
[74] T. Galatyuk *et al.* [HADES Collaboration], these proceedings.
[75] M. A. Stephanov, K. Rajagopal and E. V. Shuryak, Phys. Rev. Lett. **81** (1998) 4816.
[76] P. Braun-Munzinger, A. Rustamov and J. Stachel, Nucl. Phys. A **960** (2017) 114.
[77] A. Bzdak, R. Holzmann and V. Koch, Phys. Rev. C **94** (2016) no.6, 064907.

[78] J. Adamczewski-Musch *et al.* [HADES Collaboration], in preparation.
[79] L. Adamczyk *et al.* [STAR Collaboration], Phys. Rev. Lett. **113** (2014) 092301.
[80] B. Ling and M. A. Stephanov, Phys. Rev. C **93** (2016) no.3, 034915.
[81] X. Luo and N. Xu, arXiv:1701.02105 [nucl-ex].